On Complete Model-Based Decomposition of Polarimetric SAR Coherency Matrix Data

Yi Cui, *Member, IEEE,* Yoshio Yamaguchi, *Fellow, IEEE,* Jian Yang, *Senior Member, IEEE,* Hirokazu Kobayashi, *Senior Member, IEEE,* Sang-Eun Park, *Member, IEEE,* and Gulab Singh, *Member, IEEE*

***Abstract*—In this paper, a general scheme for complete model-based decomposition of the polarimetric synthetic aperture radar (POLSAR) coherency matrix data is presented. We show that the POLSAR coherency matrix can be completely decomposed into three components contributed by volume scattering and two single scatterers (characterized by rank-1 matrices). Under this scheme, solving for the volume scattering power amounts to a generalized eigendecomposition problem and the non-negative power constraint uniquely determines the the minimum eigenvalue as the volume scattering power. Furthermore, in order to discriminate the remaining components we propose two approaches. One is based on eigendecomposition and the other is based on model fitting, both of which are shown to properly resolve the surface and double-bounce scattering ambiguity. As a result, this paper in particular contributes to two pending needs for model-based POLSAR decomposition. Firstly, it overcomes negative power problems, i.e., all the decomposed powers are strictly guaranteed non-negative; and secondly, the three-component decomposition exactly accounts for every element of the observed coherency matrix, leading to a complete utilization of the fully polarimetric information.**

***Index Terms*—Polarimetric synthetic aperture radar (POLSAR), coherency matrix, model-based scattering power decomposition.**

I. Introduction

POLARIMETRIC synthetic aperture radar (POLSAR) is an advanced microwave remote sensing system which acquires not only high-resolution image but also complete electromagnetic scattering characteristics of the terrain targets. Therefore, polarimetric analysis of the POLSAR data has received an increasing research attention along with the launch of recent platforms such as ALOS-PALSAR, RADARSAT-2 and TerraSAR-X equipped with quad-polarization data-take capabilities.

Due to the reason that the measured scattering matrix is often affected by the noise-like speckle, incoherent analysis making use of the second-order statistics such as the coherency/covariance matrix is mostly used. Among the many methods proposed in the past decades [1]–[7], two representative groups can be identified, i.e., the eigendecomposition-based approaches and the model-based approaches, which are respectively pioneered by Cloude-Pottier [1] and Freeman-Durden [2]. However, as compared to the eigendecomposition-based method, the model-based decomposition remains an open question in at least two aspects. First, efforts are still being made for fully utilizing the polarimetric information. A complete coherency/covariance matrix contains 9 independent real-valued parameters [8]. The Freeman-Durden decomposition [2] explicitly assumes reflection symmetry and thus only accounts for 5 parameters. Yamaguchi et al [3] extends the method by adding the helix term which accounts for one more independent parameter. Later, the orientation angle compensation has also been introduced to model-based decomposition [4], [7], [9]. It is shown that this transformation equivalently reduces the independent parameters from 9 to 8 [8] such that after matrix rotation the modified Freeman-Durden decomposition can account for 5 out of 8 parameters while for modified Yamaguchi decomposition the number becomes 6 out of 8. Most recently, advancement has been made to fully use the polarimetric information within the four-component decomposition scheme [8] while as within the three-component decomposition scheme no such progress has been seen, to the best of our knowledge.

On the other hand, emergence of negative component powers has been noticed by many researches as a potential flaw that might undermine the usability of the decomposition results [3]–[5]. In order to prevent this from happening, several ad-hoc approaches have been adopted based on examination of teh decomposed powers [3], [4]. More recently, van Zyl et al [5] proposed to estimate the volume scattering power based on the constraint of nonnegative eigenvalues. It is a systematic approach which ensures that all the extracted component powers are non-negative. However, an analytically tractable solution of their method also depends on the reflection-symmetry assumption. In the case of non-reflection-symmetry, no computationally efficient algorithm has been derived yet.

This paper is then dedicated to provide a general method for simultaneously solving the aforementioned problems, especially on full utilization of the polarimetric information and prevention of negative powers. We focus on the three-component decomposition scheme and show that the POLSAR coherency matrix can be completely and exactly decomposed into three components contributed by volume scattering and two single scatterers with strictly non-negative powers. The paper is organized as follows. In Section II, a brief introduction of the three-component decomposition scheme using the coherency matrix is introduced. Section III presents the complete decomposition method, including volume scattering power

Manuscript received August 06, 2012; revised February 18, 2013; accepted April 04, 2013. The work was in part supported by the Space Sensing Project funded by the Ministry of Education of Japan and in part supported by the National Science Foundation of China (No. 41171317).

Y. Cui, Y. Yamaguchi, and H. Kobayashi are with Faculty of Engineering, Niigata University, Niigata 950-2181, Japan (e-mail: cuiyi.trea@gmail.com).

J. Yang is with Department of Electronic Engineering, Tsinghua University, Beijing 100084, China.

S.-E. Park and G. Singh are with Graduate School of Science and Technology, Niigata University, Niigata 950-2181, Japan.

extraction and single scatterer discrimination. Experimental results with real POLSAR data are given in Section IV and Section V concludes the paper. Mathematical proofs and derivations are shown in Appendices.

II. POLSAR Coherency Matrix and Three-Component Decomposition Scheme

A. POLSAR Coherency Matrix

In model-based POLSAR decomposition, various literatures have witnessed the use of two data formats, commonly known as the coherency matrix [3], [4], [7] and the covariance matrix [2], [5], [6]. From a statistical point of view, both the coherency matrix and covariance matrix represent second-order statistics of the polarimetric information and they are equivalent to each other up to orthogonal transformations. In this paper we focus on decomposing the coherency matrix as its covariance matrix counterpart can be straightforwardly analogized. By definition, the coherency matrix is given by:

$$\mathbf{T} = \mathbb{E}\left(\mathbf{k}_{\mathrm{p}}\mathbf{k}_{\mathrm{p}}^{\mathrm{H}}\right), \tag{1}$$

where $\mathbb{E}$ denotes mathematical expectation and the superscript H stands for the conjugate transpose operator. The Pauli-vector $\mathbf{k}_{\mathrm{p}}$ is defined as:

$$\mathbf{k}_{\mathrm{p}} = \frac{1}{\sqrt{2}}\begin{bmatrix} S_{\mathrm{HH}} + S_{\mathrm{VV}} \\ S_{\mathrm{HH}} - S_{\mathrm{VV}} \\ 2S_{\mathrm{HV}} \end{bmatrix}, \tag{2}$$

where S_{HH}, S_{VV}, and S_{HV} are elements of the polarimetric scattering matrix. According to (1), procurement of the coherency matrix is in fact an estimation problem which can be cast into the general setting of POLSAR data filtering [10]. Although different filtering/reconstructing methods will definitely affect the estimation accuracy of the coherency matrix and consequently the decomposition result thereupon, detailed discussion is beyond the scope of this paper. As within this paper, the coherency matrix can be obtained by ensemble averaging [8] or filtering [10] and the estimation uncertainty are also reflected in the decomposed powers.

B. Three-Component Decomposition Scheme Based on Coherency Matrix

Under the three-component decomposition scheme, the effort is to expand the measured coherency matrix, $\mathbf{T}$, as a linear combination of three submatrices corresponding to surface scattering, double-bounce scattering, and volume scattering mechanisms [2]. Mathematically, the relation can be written as:

$$\mathbf{T} = P_{\mathrm{S}}\mathbf{T}_{\mathrm{S}} + P_{\mathrm{D}}\mathbf{T}_{\mathrm{D}} + P_{\mathrm{V}}\mathbf{T}_{\mathrm{V}}, \tag{3}$$

where $\mathbf{T}_{\mathrm{S}}$, $\mathbf{T}_{\mathrm{D}}$, and $\mathbf{T}_{\mathrm{V}}$ are the coherency matrices accounting for surface scattering, double-bounce scattering, and volume scattering, respectively; P_{S}, P_{D}, and P_{V} are expansion coefficients. Throughout this paper $\mathbf{T}_{\mathrm{S}}$, $\mathbf{T}_{\mathrm{D}}$, and $\mathbf{T}_{\mathrm{V}}$ are always power normalized such that P_{S}, P_{D}, and P_{V} represent power contributions which by physical meaning shall be all non-negative numbers.

Solving the matrix expansion problem of (3) starts with modeling (parameterizing) $\mathbf{T}_{\mathrm{S}}$, $\mathbf{T}_{\mathrm{D}}$, and $\mathbf{T}_{\mathrm{V}}$. For example, in the Freeman-Durden decomposition the following (power normalized) coherency matrices are used [2]:

$$\mathbf{T}_{\mathrm{S}}(\beta) = \frac{1}{1+|\beta|^2}\begin{bmatrix} 1 & \beta^* & 0 \\ \beta & |\beta|^2 & 0 \\ 0 & 0 & 0 \end{bmatrix}, |\beta| < 1, \tag{4}$$

$$\mathbf{T}_{\mathrm{D}}(\alpha) = \frac{1}{1+|\alpha|^2}\begin{bmatrix} |\alpha|^2 & \alpha^* & 0 \\ \alpha & 1 & 0 \\ 0 & 0 & 0 \end{bmatrix}, |\alpha| < 1, \tag{5}$$

$$\mathbf{T}_{\mathrm{V}} = \frac{1}{4}\begin{bmatrix} 2 & 0 & 0 \\ 0 & 1 & 0 \\ 0 & 0 & 1 \end{bmatrix}, \tag{6}$$

where the unknown parameters α and β together with the expansion coefficients, $P_{\mathrm{S}}, P_{\mathrm{D}}, P_{\mathrm{V}}$, are to be determined from (3). However, the above models assume reflection symmetry of the media and consequently cannot fully explain the scattering mechanisms present in the measured coherency matrix. For example, it is clear from (4)–(6) that the elements T_{13} and T_{23} of $\mathbf{T}$ will not be accounted for whatsoever. In addition, directly solving the unknown parameters does not always guarantee physically meaningful outcomes (e.g., positive component powers), due to model mismatch or measurement uncertainty (speckle noise) [11]. In order to overcome these difficulties, in the next section we will cast the matrix expansion problem under a more general scheme and show how exact solutions can be found therein.

III. Complete Three-Component Decomposition of POLSAR Coherency Matrix

In this section, we solve the matrix expansion problem of (3) under the following conditions:

- Condition #1: $\mathbf{T}_{\mathrm{V}}$ is a known positive-definite Hermitian matrix.
- Condition #2: $\mathbf{T}_{\mathrm{S}}$ and $\mathbf{T}_{\mathrm{D}}$ are two unknown single-rank matrices.
- Condition #3: $P_{\mathrm{S}}, P_{\mathrm{D}}, P_{\mathrm{V}}$ are unknown non-negative expansion coefficients.

It should be noted that in Condition #1 we do not designate any specific form for $\mathbf{T}_{\mathrm{V}}$ but only specify the positive-definiteness. In fact, it can be shown that (see Appendix A) that for any volume matrix generated from a cloud of random scatterers, this condition will be generally satisfied. As a result, existing volume scattering models [3], [6], [12], [13] can be all safely used. Condition #2 is a generalization of the surface and double-bounce scatterers based on the observation that both (4) and (5) are special rank-1 matrices. Also in Condition #3 we emphasize the non-negativeness of the expansion coefficients because it is this solution that is physically meaningful. Accordingly, the observed POLSAR coherency matrix is assumed to be the combined contribution of volume scattering and two single scatterers. Note, however, that although we keep the conventional subscript notation for $\mathbf{T}_{\mathrm{S}}$ and $\mathbf{T}_{\mathrm{D}}$, they do not necessarily stand for simple surface and double-bounce scattering anymore. As will be seen in Section III-B, there

exists ambiguity with regard to discrimination of these two components and explanation of their underlying mechanisms depends on further analysis for a given solution.

A. Solving for Volume Scattering Component

First we rewrite (3) by:

$$\mathbf{T} - P_{\mathrm{V}}\mathbf{T}_{\mathrm{V}} = P_{\mathrm{S}}\mathbf{T}_{\mathrm{S}} + P_{\mathrm{D}}\mathbf{T}_{\mathrm{D}}. \tag{7}$$

Since both $\mathbf{T}_{\mathrm{S}}$ and $\mathbf{T}_{\mathrm{D}}$ are rank-1 matrices (Condition #2), $\mathbf{T} - P_{\mathrm{V}}\mathbf{T}_{\mathrm{V}}$ is at most a rank-2 matrix. Consequently, the determinant of $\mathbf{T} - P_{\mathrm{V}}\mathbf{T}_{\mathrm{V}}$ is bound to vanish, that is:

$$\det(\mathbf{T} - P_{\mathrm{V}}\mathbf{T}_{\mathrm{V}}) = 0, \tag{8}$$

where $\det(\cdot)$ denotes matrix determinant. It can be shown (see Appendix B) that (8) is a simple cubic equation about P_{V} whose three roots can be easily obtained. However, before the volume scattering power can be determined, two issues require resolution: 1) whether non-negative roots exist for (8); and 2) if non-negative roots exist, which one of them applies for P_{V}.

Answering these questions relies on the observation that the roots of (8) in fact correspond to the following generalized eigendecomposition problem:

$$\mathbf{T}\mathbf{x} = \lambda\mathbf{T}_{\mathrm{V}}\mathbf{x}, \tag{9}$$

where λ is the generalized eigenvalue and $\mathbf{x}$ is the associated eigenvector. In Appendix C we have proved that under the condition that $\mathbf{T}_{\mathrm{V}}$ is positive-definite and Hermitian (Condition #1), all the eigenvalues of (9) are non-negative for any positive-semidefinite Hermitian matrix $\mathbf{T}$. Therefore, all the roots of (8) are non-negative.

In order to determine which one of the roots represents the volume scattering power, we note that the single-rankness of $\mathbf{T}_{\mathrm{S}}$ and $\mathbf{T}_{\mathrm{D}}$ (Condition #2) implies that they can be written as:

$$\mathbf{T}_{\mathrm{S}} = \mathbf{k}_{\mathrm{S}}\mathbf{k}_{\mathrm{S}}^{\mathrm{H}}, \tag{10}$$

$$\mathbf{T}_{\mathrm{D}} = \mathbf{k}_{\mathrm{D}}\mathbf{k}_{\mathrm{D}}^{\mathrm{H}}, \tag{11}$$

where $\mathbf{k}_{\mathrm{S}}$ and $\mathbf{k}_{\mathrm{S}}$ are the corresponding Pauli-vectors. Thus the non-negativeness of P_{S} and P_{D} (Condition #3) dictates that $\mathbf{T} - P_{\mathrm{V}}\mathbf{T}_{\mathrm{V}}$ be positive-semidefinite because for any vector $\mathbf{y}$ we have:

$$\begin{aligned}\mathbf{y}^{\mathrm{H}}(\mathbf{T} - P_{\mathrm{V}}\mathbf{T}_{\mathrm{V}})\mathbf{y} &= \mathbf{y}^{\mathrm{H}}(P_{\mathrm{S}}\mathbf{T}_{\mathrm{S}} + P_{\mathrm{D}}\mathbf{T}_{\mathrm{D}})\mathbf{y} \\ &= P_{\mathrm{S}}\left|\mathbf{y}^{\mathrm{H}}\mathbf{k}_{\mathrm{S}}\right|^2 + P_{\mathrm{D}}\left|\mathbf{y}^{\mathrm{H}}\mathbf{k}_{\mathrm{D}}\right|^2 \\ &\geq 0.\end{aligned} \tag{12}$$

In Appendix D, we have proved that $\mathbf{T} - P_{\mathrm{V}}\mathbf{T}_{\mathrm{V}}$ is positive-semidefinite if and only if $P_{\mathrm{V}} = \lambda_{\min}$ where $\lambda_{\min}$ is the minimum generalized eigenvalue of (9). Hence the volume scattering power is uniquely determined as equal to the minimum root of (8).

It is worth mentioning that from the perspective of non-negative eigenvalue decomposition (NNED) [5], the minimum root of (8) can be also considered as the maximum value possible for the volume scattering. If P_{V} takes a smaller value, the remaining matrix, $\mathbf{T} - P_{\mathrm{V}}\mathbf{T}_{\mathrm{V}}$, will become strictly positive-definite. This consequently leads to a four-component model of volume scattering and up to three single scatterers. However, using the maximum amount of power results in the best fit of the volume scattering model to the measured coherency matrix and has been suggested as a reasonable strategy [5], [6]. In addition, van Zyl et al [5] proposed an alternative approach to obtain the maximum possible volume power by deriving the eigenvalues of the remaining matrix but the analytical solution is only available when reflection-symmetry holds. On the other hand, it has been shown here that for the general case of non-reflection-symmetry, the volume strength is also analytically tractable through solving the cubic equation of (8) or the generalized eigendecomposition problem of (9).

B. Discriminating Single Scatterers by Eigendecomposition

The remaining matrix, $\mathbf{T}' = \mathbf{T} - P_{\mathrm{V}}\mathbf{T}_{\mathrm{V}}$, contains the contribution of up to two single scatterers and the next purpose is to discriminate them. However, there exist infinite ways in terms of writing $\mathbf{T}'$ as the sum of two rank-1 matrices because we are handling a problem with more unknowns than the number of equations. To be more specific, we can write the corresponding Pauli-vectors, $\mathbf{k}_{\mathrm{S}}$ and $\mathbf{k}_{\mathrm{D}}$, in the following normalized forms:

$$\mathbf{k}_{\mathrm{S}}(\delta_{\mathrm{S}}, \omega_{\mathrm{S}}, \phi_{\mathrm{S}}, \varphi_{\mathrm{S}}) = \begin{bmatrix}\cos\delta_{\mathrm{S}} \\ \sin\delta_{\mathrm{S}}\cos\omega_{\mathrm{S}}e^{j\phi_{\mathrm{S}}} \\ \sin\delta_{\mathrm{S}}\sin\omega_{\mathrm{S}}e^{j\varphi_{\mathrm{S}}}\end{bmatrix}, \tag{13}$$

$$\mathbf{k}_{\mathrm{D}}(\delta_{\mathrm{D}}, \omega_{\mathrm{D}}, \phi_{\mathrm{D}}, \varphi_{\mathrm{D}}) = \begin{bmatrix}\cos\delta_{\mathrm{D}} \\ \sin\delta_{\mathrm{D}}\cos\omega_{\mathrm{D}}e^{j\phi_{\mathrm{D}}} \\ \sin\delta_{\mathrm{D}}\sin\omega_{\mathrm{D}}e^{j\varphi_{\mathrm{D}}}\end{bmatrix}, \tag{14}$$

where $\delta_{\mathrm{S}}, \omega_{\mathrm{S}}, \phi_{\mathrm{S}}, \varphi_{\mathrm{S}}, \delta_{\mathrm{D}}, \omega_{\mathrm{D}}, \phi_{\mathrm{D}}, \varphi_{\mathrm{D}}$ are unknown real angles. Then together with the unknown power coefficients P_{S} and P_{D}, we have a total of 10 free variables, whereas the maximum number of independent equations available from $\mathbf{T}'$ is 8 (but not 9 because $\det(\mathbf{T}') = 0$ reduces one dimension of the data). Unique solution is only possible with further assumptions.

Based on the fact that $\mathbf{T}'$ is a positive-semidefinite matrix, an immediate way to write $\mathbf{T}'$ as the sum of two rank-1 matrices with positive expansion coefficients would be by the eigendecomposition:

$$\mathbf{T}' = \lambda_1\mathbf{k}_1\mathbf{k}_1^{\mathrm{H}} + \lambda_2\mathbf{k}_2\mathbf{k}_2^{\mathrm{H}}, \tag{15}$$

where without loss of generality we assume $\lambda_1 \geq \lambda_2$. In fact, eigendecomposition implicitly assumes the orthogonality between $\mathbf{k}_1$ and $\mathbf{k}_2$ which adds two more equations (respectively from the real and imaginary parts) such that (15) becomes a unique solution. For any positive-semidefinite Hermitian matrix, its eigendecomposition is equivalent to single value decomposition (SVD). Then $\lambda_1\mathbf{k}_1\mathbf{k}_1^{\mathrm{H}}$ is the optimal rank-1 approximation for $\mathbf{T}'$ in the sense of minimum Frobenius distance [14]. Hence $\mathbf{k}_1$ in fact stands for the predominant single scatterer and $\mathbf{k}_2$ is the minor scatterer. Consequently, eigendecomposition can be considered as dominant scattering decomposition for the remaining matrix.

In order further interpret the scattering mechanisms underlying $\mathbf{k}_1$ and $\mathbf{k}_2$, we follow van Zyl's reasoning by inspecting the co-polarized phase [5], [15]. However, a closer examination can also consider the orientation of each single scatterer. Let $\mathbf{S}_i$

be the scattering matrix corresponding to $\mathbf{k}_i$. Then according to the Huynen decomposition [16] $\mathbf{S}_i$ can be de-oriented as:

$$\mathbf{S}_i' = \mathfrak{R}(-\tau_i)\mathbf{S}_i\mathfrak{R}(\tau_i), \tag{16}$$

where τ_i is the orientation angle (see Appendix E for its derivation) and the transformation $\mathfrak{R}(\tau_i)$ is given by:

$$\mathfrak{R}(\tau_i) = \begin{bmatrix}\cos(\tau_i) & -\sin(\tau_i)\\ \sin(\tau_i) & \cos(\tau_i)\end{bmatrix}. \tag{17}$$

Finally we check the co-polarized phase of $\mathbf{S}_i'$ to determine whether even or odd scattering is present.

To summarize, the procedure for power decomposition of the measured coherency matrix into surface, double-bounce and volume scattering is outlined in Algorithm 1.

Algorithm 1

Input: $\mathbf{T}$ and $\mathbf{T}_\mathrm{V}$
Solve cubic equation: $\det(\mathbf{T} - x\mathbf{T}_\mathrm{V}) = 0 \Rightarrow x_1, x_2, x_3$
Determine volume power: $P_\mathrm{V} = \min\{x_1, x_2, x_3\}$
Obtain remaining matrix: $\mathbf{T}' = \mathbf{T} - P_\mathrm{V}\mathbf{T}_\mathrm{V}$
Perform eigendecomposition: $\mathbf{T}' = \lambda_1\mathbf{k}_1\mathbf{k}_1^\mathrm{H} + \lambda_2\mathbf{k}_2\mathbf{k}_2^\mathrm{H}$
for $i = 1$ to 2 **do**
  Write $\mathbf{S}_i$ in terms of Pauli-vector $\mathbf{k}_i$
  Obtain orientation angle τ_i of $\mathbf{S}_i$
  Perform de-orientation: $\mathbf{S}_i' = \mathfrak{R}(-\tau_i)\mathbf{S}_i\mathfrak{R}(\tau_i)$
  if $\mathrm{Re}\left\{S_{i,\mathrm{HH}}'\left(S_{i,\mathrm{VV}}'\right)^*\right\} > 0$ **then**
    $P_\mathrm{S} \leftarrow P_\mathrm{S} + \lambda_i$
  else
    $P_\mathrm{D} \leftarrow P_\mathrm{D} + \lambda_i$
  end if
end for
Output: $P_\mathrm{S}, P_\mathrm{D}, P_\mathrm{V}$

C. Discriminating Single Scatterers by Model Fitting

As previously pointed out, there exist an infinite number ways in terms of writing $\mathbf{T}'$ as the sum of two rank-1 matrices and the eigendecomposition in Section III-B offers just one of them. In this sub-section, we provide another solution with a model-based approach.

In particular, we seek to fit a Bragg scatterer subject to azimuth slope modulation [17] to $\mathbf{T}'$. The coherency matrix for such a scatterer can be written as:

$$\mathbf{T}_\mathrm{S}(\beta, \theta) = \mathbf{R}^\mathrm{T}(\theta) \cdot \mathbf{T}_\mathrm{S}(\beta) \cdot \mathbf{R}(\theta), \tag{18}$$

where $\mathbf{T}_\mathrm{S}(\beta)$ is given in (4) and θ denotes the orientation angle. The rotation matrix $\mathbf{R}(\theta)$ is given by:

$$\mathbf{R}(\theta) = \begin{bmatrix}1 & 0 & 0\\ 0 & \cos 2\theta & \sin 2\theta\\ 0 & -\sin 2\theta & \cos 2\theta\end{bmatrix}. \tag{19}$$

Then after rotation compensation by $\mathbf{T}'(\theta) = \mathbf{R}(\theta)\mathbf{T}'\mathbf{R}^\mathrm{T}(\theta)$, we can arrive at the model equation shown in (20) at the bottom of this page where $\delta, \omega, \phi, \varphi$ are the re-normalized vector parameters of $\mathbf{k} = \mathbf{R}(\theta)\mathbf{k}_\mathrm{D}(\delta_\mathrm{D}, \omega_\mathrm{D}, \phi_\mathrm{D}, \varphi_\mathrm{D})$. The unknowns on the right-hand side of (20) can be directly solved in terms of the elements of $\mathbf{T}'(\theta)$ and the results are given by:

$$P_\mathrm{S} = T_{11}'(\theta) + T_{22}'(\theta) - \frac{|T_{13}'(\theta)|^2 + |T_{23}'(\theta)|^2}{T_{33}'(\theta)}, \tag{21a}$$

$$\beta = \frac{T_{33}'(\theta)[T_{12}'(\theta)]^* - T_{23}'(\theta)[T_{13}'(\theta)]^*}{T_{11}'(\theta)T_{33}'(\theta) - |T_{13}'(\theta)|^2}, \tag{21b}$$

$$P_\mathrm{D} = T_{33}'(\theta) + \frac{|T_{13}'(\theta)|^2 + |T_{23}'(\theta)|^2}{T_{33}'(\theta)}, \tag{21c}$$

$$\delta = \sin^{-1}\sqrt{\frac{|T_{33}'(\theta)|^2 + |T_{23}'(\theta)|^2}{|T_{33}'(\theta)|^2 + |T_{23}'(\theta)|^2 + |T_{13}'(\theta)|^2}}, \tag{21d}$$

$$\omega = \sin^{-1}\sqrt{\frac{|T_{33}'(\theta)|^2}{|T_{33}'(\theta)|^2 + |T_{23}'(\theta)|^2}}, \tag{21e}$$

$$\phi = \arg\left\{T_{23}'(\theta)[T_{13}'(\theta)]^*\right\}, \tag{21f}$$

$$\varphi = -\arg\left[T_{13}'(\theta)\right], \tag{21g}$$

where the superscript * denotes the conjugate of a complex number and $\arg[\cdot]$ denotes the argument. From (21) it can be verified that the component powers, P_S and P_D, are both strictly non-negative. $P_\mathrm{D} \geq 0$ is obvious in (21c). As for the non-negativity of P_S, according to the positive-semidefiniteness of $\mathbf{T}'(\theta)$ any of its principal minors should be also positive-semidefinite. This property leads to the following inequalities:

$$T_{11}'(\theta)T_{33}'(\theta) - |T_{13}'(\theta)|^2 \geq 0, \tag{22a}$$

$$T_{22}'(\theta)T_{33}'(\theta) - |T_{23}'(\theta)|^2 \geq 0, \tag{22b}$$

From the above equation it is easy to see that P_S in (21a) is also non-negative.

Next, note in (21) that all the model parameters and power coefficients are functions of θ. Then we obtain the optimal value of θ such that P_S is maximized. Physically, it means we try to fit the best model $\mathbf{T}_\mathrm{S}(\beta, \theta)$ to the remaining matrix $\mathbf{T}'$. The solution to this optimization problem is (see Appendix F for derivation):

$$\theta_\mathrm{max} = \frac{1}{4}\left[\tan^{-1}\frac{\left(B + \sqrt{B^2 - C}\right)d - a}{\left(B + \sqrt{B^2 - C}\right)e - b} + k\pi\right], \tag{23}$$

where $k = 0$ or $k = 1$ accounts for the angle ambiguity and can be determined according to (F.8) (see Appendix F). The constants on the right hand side of (23) are respectively given by:

$$B = \frac{ad + eb - cf}{d^2 + e^2 - f^2}, \tag{24a}$$

$$\mathbf{T}'(\theta) = \frac{P_\mathrm{S}}{1 + |\beta|^2}\begin{bmatrix}1 & \beta^* & 0\\ \beta & |\beta|^2 & 0\\ 0 & 0 & 0\end{bmatrix} + P_\mathrm{D}\begin{bmatrix}\cos^2\delta & \cos\delta\sin\delta\cos\omega e^{-j\phi} & \cos\delta\sin\delta\sin\omega e^{-j\varphi}\\ \cos\delta\sin\delta\cos\omega e^{j\phi} & \sin^2\delta\cos^2\omega & \sin^2\delta\cos\omega\sin\omega e^{j(\phi-\varphi)}\\ \cos\delta\sin\delta\sin\omega e^{j\varphi} & \sin^2\delta\cos\omega\sin\omega e^{j(\varphi-\phi)} & \sin^2\delta\sin^2\omega\end{bmatrix} \tag{20}$$

$$C = \frac{a^2 + b^2 - c^2}{d^2 + e^2 - f^2}, \tag{24b}$$

$$a = \frac{1}{2}\left(T'_{11}T'_{33} - |T'_{13}|^2 - T'_{11}T'_{22} + |T'_{12}|^2\right), \tag{24c}$$

$$b = \mathrm{Re}\left[T'_{12}\left(T'_{13}\right)^*\right] - T'_{11}\mathrm{Re}\left(T'_{23}\right), \tag{24d}$$

$$c = T'_{22}T'_{33} - |T'_{23}|^2 + \frac{1}{2}\left(T'_{11}T'_{33} - |T'_{13}|^2 + T'_{11}T'_{22} - |T'_{12}|^2\right), \tag{24e}$$

$$d = \frac{1}{2}\left(T'_{33} - T'_{22}\right), \tag{24f}$$

$$e = -\mathrm{Re}\left(T'_{23}\right), \tag{24g}$$

$$f = \frac{1}{2}\left(T'_{22} + T'_{33}\right). \tag{24h}$$

Finally we substitute $\theta_{\max}$ to (21b) for model validation because Bragg scattering requires $|\beta| < 1$. However, if $|\beta| > 1$, then in this case we are in fact fitting a rotated dihedral scatterer to the remaining matrix. The scattering mechanism for the other single scatterer can be also interpreted in the same way as in Section III-B, that is, we perform the Huynen decomposition and check the co-polarized phase of the de-oriented scattering matrix for odd or even scattering. To summarize, the aforementioned decomposition procedure is restated in Algorithm 2.

Algorithm 2

Input: $\mathbf{T}$ and $\mathbf{T}_{\mathrm{V}}$
Solve cubic equation: $\det(\mathbf{T} - x\mathbf{T}_{\mathrm{V}}) = 0 \Rightarrow x_1, x_2, x_3$
Determine volume power: $P_{\mathrm{V}} = \min\{x_1, x_2, x_3\}$
Obtain remaining matrix: $\mathbf{T}' = \mathbf{T} - P_{\mathrm{V}}\mathbf{T}_{\mathrm{V}}$
Determine a, b, c, d, e, f, B, C by (24)
Obtain orientation angle θ by (23)
Rotate remaining matrix: $\mathbf{T}'(\theta) = \mathbf{R}(\theta)\mathbf{T}\mathbf{R}^{\mathrm{T}}(\theta)$
$P_{\mathrm{S}} = 0, P_{\mathrm{D}} = 0$
Calculate β by (21b)
if $|\beta| < 1$ **then**
    $P_{\mathrm{S}} \leftarrow P_{\mathrm{S}} + T'_{11}(\theta) + T'_{22}(\theta) - \frac{|T'_{13}(\theta)|^2 + |T'_{23}(\theta)|^2}{T'_{33}(\theta)}$
else
    $P_{\mathrm{D}} \leftarrow P_{\mathrm{D}} + T'_{11}(\theta) + T'_{22}(\theta) - \frac{|T'_{13}(\theta)|^2 + |T'_{23}(\theta)|^2}{T'_{33}(\theta)}$
end if
Calculate $\delta, \omega, \phi, \varphi$ by (21d)–(21g)
$\mathbf{k} = \left[\cos\delta, \sin\delta\cos\omega e^{j\phi}, \sin\delta\sin\omega e^{j\varphi}\right]^{\mathrm{T}}$
Write $\mathbf{S}$ in terms of Pauli-vector $\mathbf{k}$
Obtain orientation angle τ of $\mathbf{S}$
Perform de-orientation: $\mathbf{S}' = \mathfrak{R}(-\tau)\mathbf{S}\mathfrak{R}(\tau)$
if $\mathrm{Re}\left\{S'_{\mathrm{HH}}\left(S'_{\mathrm{VV}}\right)^*\right\} > 0$ **then**
    $P_{\mathrm{S}} \leftarrow P_{\mathrm{S}} + T'_{33}(\theta) + \frac{|T'_{13}(\theta)|^2 + |T'_{23}(\theta)|^2}{T'_{33}(\theta)}$
else
    $P_{\mathrm{D}} \leftarrow P_{\mathrm{D}} + T'_{33}(\theta) + \frac{|T'_{13}(\theta)|^2 + |T'_{23}(\theta)|^2}{T'_{33}(\theta)}$
end if
Output: $P_{\mathrm{S}}, P_{\mathrm{D}}, P_{\mathrm{V}}$

IV. Decomposition Results with Selected Experimental Scenes

In this section, we present the decomposition results for POLSAR data collected by the NASA/JPL AIRSAR, JAXA ALOS-PALSAR and CSA/MDA RASARSAT-2. We compare the proposed methods with the Freeman-Durden decomposition (FDD) [2], the Yamaguchi four-component decomposition with rotation compensation (Y4R) [7], and the non-negative eigenvalue decomposition assuming reflection symmetry (NNED-RS) with maximum volume scattering power [5]. In addition, throughout this section we have tested, for Algorithm 1, Algorithm 2, and NNED-RS, a library of three volume models that are representative of the horizontally, uniformly, and vertically oriented cloud of dipoles. The coherency matrices are respectively given by [3]:

$$\mathbf{T}_{\mathrm{V}}^{\mathrm{horizontal}} = \frac{1}{30}\begin{bmatrix} 15 & 5 & 0 \\ 5 & 7 & 0 \\ 0 & 0 & 8 \end{bmatrix}, \tag{25a}$$

$$\mathbf{T}_{\mathrm{V}}^{\mathrm{uniform}} = \frac{1}{4}\begin{bmatrix} 2 & 0 & 0 \\ 0 & 1 & 0 \\ 0 & 0 & 1 \end{bmatrix}, \tag{25b}$$

$$\mathbf{T}_{\mathrm{V}}^{\mathrm{vertical}} = \frac{1}{30}\begin{bmatrix} 15 & -5 & 0 \\ -5 & 7 & 0 \\ 0 & 0 & 8 \end{bmatrix}. \tag{25c}$$

We then compute the power for each of the aforementioned volume models and choose the one with the largest strength as the best model.

A. Study Scene 1: Volume Scattering Dominant Area

We first test on the L-band AIRSAR polarimetric data acquired over the Black Forest in Germany where random volume scattering is expected to be dominant. A spatial multi-look processing by combining 5×5 (range×azimuth) neighboring pixels is performed on this dataset in order to achieve a better coherency matrix estimate. Fig. 1 displays the power decomposition results using five methods. It shows that while all the methods confirm the volume scattering dominance in the vegetated area, different scattering powers are obtained. The power distributions in the selected patches in Fig. 1 are shown in Fig. 2. It can be seen that Algorithm 1 and Algorithm 2 give the least volume scattering power estimation. In particular, it is interesting to note in Fig. 2(a)–(c) that the proposed methods extract smaller volume scattering power than the NNED-RS. Recall that the former can be also regarded as NNED but without assuming reflection symmetry. Thus the power differences in Fig. 2(a)–(c) indicate that taking account of non-reflection-symmetry will further reduce the volume scattering power. This appears to be a reasonable result given that the volume models used in (25) are not characterized by non-reflection-symmetric terms.

In order to see which one of the volume models in (25) produces the best fit to the scene, we display the maps of model selection in Fig. 3, where Fig. 3(a) is the map generated by fitting the volume model to the complete coherency matrix and Fig. 3(b) is the map generated by fitting the volume model

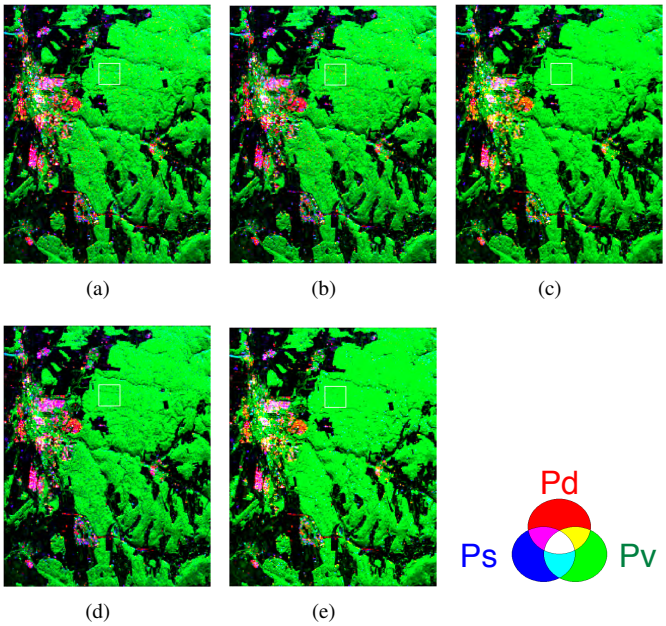

Fig. 1. Decomposition results of the AIRSAR data by (a) Algorithm 1, (b) Algorithm 2, (c) non-negative eigenvalue decomposition assuming reflection symmetry, (d) Yamaguchi decomposition with rotation angle compensation, and (e) Freeman-Durden decomposition. Power distributions in the selected boxes containing vegetated areas are shown in Fig. 2.

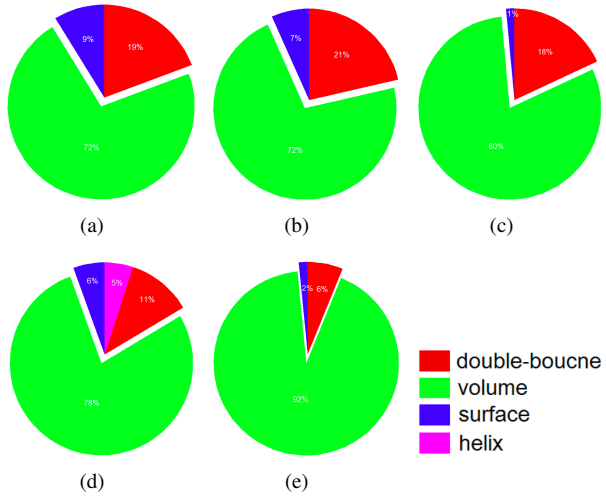

Fig. 2. Power distributions in the selected boxes in Fig. 1 of the decomposition results by (a) Algorithm 1, (b) Algorithm 2, (c) non-negative eigenvalue decomposition assuming reflection symmetry, (d) Yamaguchi decomposition with rotation angle compensation, and (e) Freeman-Durden decomposition.

to the coherency matrix assuming reflection symmetry. It is interesting to note that both Fig. 3(a) and Fig. 3(b) nicely delineate the forested area that is best modeled by the horizontally oriented dipoles. Alternatively, Yamaguchi et al [3] suggested that the volume models can be chosen from based on the magnitude balance of $\langle|S_{\rm HH}|^2\rangle$ and $\langle|S_{\rm VV}|^2\rangle$. Specifically, if $10\lg\left(\langle|S_{\rm HH}|^2\rangle/\langle|S_{\rm VV}|^2\rangle\right) < -2\text{dB}$, $\mathbf{T}_{\rm V}^{\rm horizontal}$ will be selected; if $10\lg\left(\langle|S_{\rm HH}|^2\rangle/\langle|S_{\rm VV}|^2\rangle\right) > -2\text{dB}$, $\mathbf{T}_{\rm V}^{\rm vertical}$ will be selected; otherwise, $\mathbf{T}_{\rm V}^{\rm uniform}$ is selected. Based on this rule, we have also plotted the map of volume model selection in Fig. 3(c). Similarity can be observed among Fig. 3(a), (b) and (c). This suggests that the volume model selection with a best

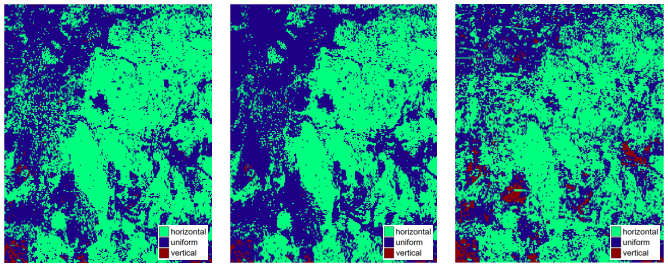

Fig. 3. Maps of volume model selection by (a) fitting the volume models to the complete coherency matrix, (b) fitting the volume models to the coherency matrix assuming reflection symmetry, and (c) magnitude balance of co-polarized channels.

fitting approach can be a useful complement to that based on prior experimental evidences.

B. Study Scene 2: Oblique Urban Area

The next test dataset is acquired by ALOS-PALSAR over the area of Kyoto on April 9, 2009. The original data format is single-look complex (SLC) scattering matrix. An ensemble averaging of 4×24 (range×azimuth) pixels is performed for estimating the coherency matrix. The resolution of the final image corresponds to 60m in the ground area. The illuminated scene mainly consists of oblique urban areas that are not orthogonal to the radar line-of-sight. The decomposition results are shown in Fig. 4. Patches containing oblique man-made structures are selected in Fig. 4 and the power distributions therein are drawn in Fig. 5. First, it can be seen in Fig. 5(e) that the FDD produced a volume scattering dominant result. This is because the FDD treats all the cross-polarization returns as volume scattering contribution and so cannot discriminate the cross-polarization power generated by oriented single scatterers such as oriented dihedrals. The NNED-RS presents an improvement with a reduced volume scattering power but the difference is subtle. This may be due to the fact that in oblique urban areas the non-reflection symmetry terms such as T_{23} can play a significant role. On the other hand, more reasonable results are achieved by Algorithm 1, Algorithm 2, and Y4R. It can be seen in Fig. 5(a), (b), (d) that both double-bounce and surface scattering powers become dominant which is more consistent with the situation in urban areas.

C. Study Scene 3: Surface Scattering Dominant Area

The third test image is acquired by RADARSAT-2 at the south of Yanliang City of Shaanxi Province in China on February 28, 2009. The original data format is also SLC with an approximate 5 meter spacing in both range and azimuth directions. Spatial multilooking is performed by combining 9×9 pixels to obtain the coherency matrix data. Fig. 6 shows the decomposition results from which we can see that surface scattering dominance is confirmed in the center of the image near the bank of a river (Wei River) by different methods. This area mainly consists of farmlands but at the time of the data acquisition (late February) no crop has been yet planted such that single-bounce scattering by bare soil is

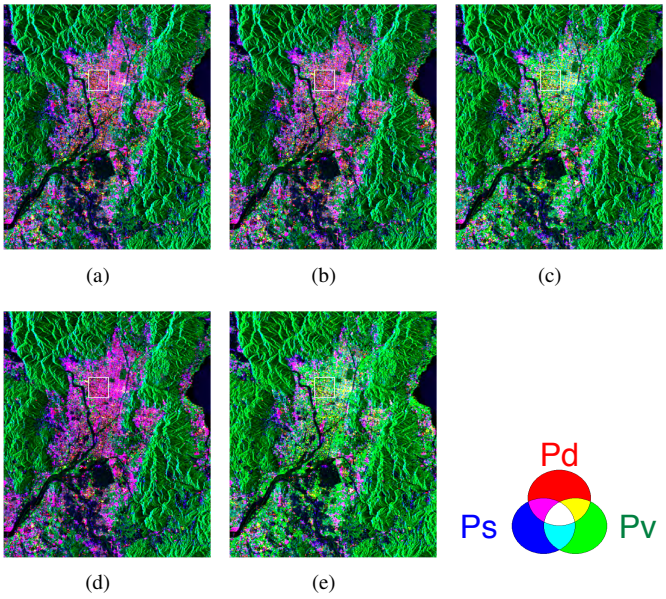

Fig. 4. Decomposition results of the ALOS-PALSAR data by (a) Algorithm 1, (b) Algorithm 2, (c) non-negative eigenvalue decomposition assuming reflection symmetry, (d) Yamaguchi decomposition with rotation angle compensation, and (e) Freeman-Durden decomposition. Power distributions in the selected boxes containing vegetated areas are shown in Fig. 5.

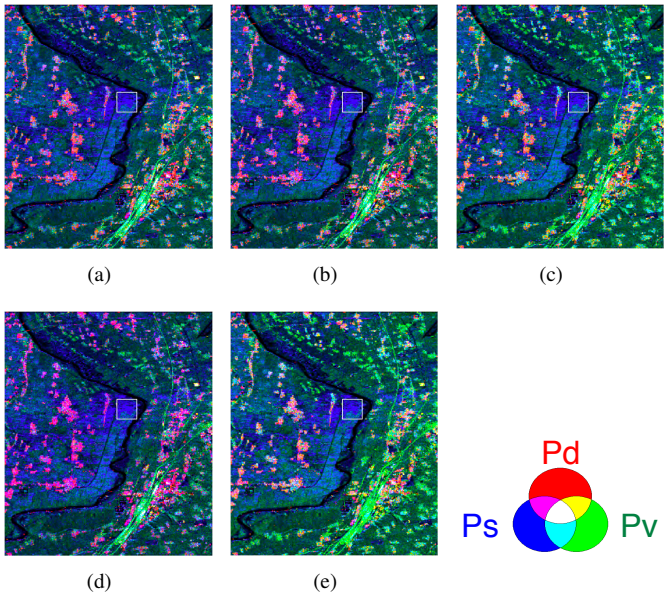

Fig. 6. Decomposition results of the RADARSAT-2 data by (a) Algorithm 1, (b) Algorithm 2, (c) non-negative eigenvalue decomposition assuming reflection symmetry, (d) Yamaguchi decomposition with rotation angle compensation, and (e) Freeman-Durden decomposition. Power distributions in the selected boxes containing vegetated areas are shown in Fig. 7.

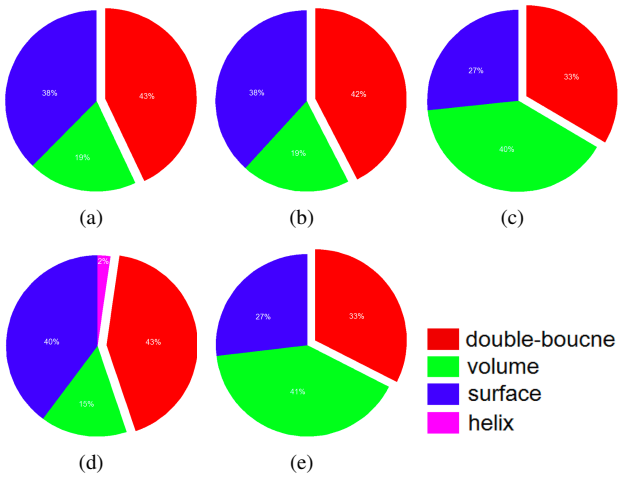

Fig. 5. Power distributions in the selected boxes in Fig. 4 of the decomposition results by (a) Algorithm 1, (b) Algorithm 2, (c) non-negative eigenvalue decomposition assuming reflection symmetry, (d) Yamaguchi decomposition with rotation angle compensation, and (e) Freeman-Durden decomposition.

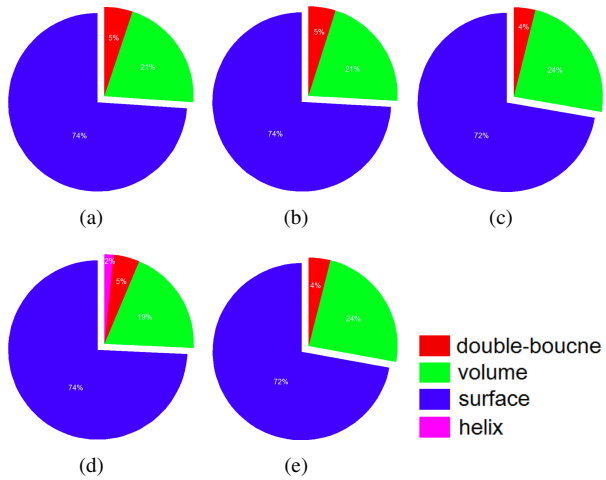

Fig. 7. Power distributions in the selected boxes in Fig. 6 of the decomposition results by (a) Algorithm 1, (b) Algorithm 2, (c) non-negative eigenvalue decomposition assuming reflection symmetry, (d) Yamaguchi decomposition with rotation angle compensation, and (e) Freeman-Durden decomposition.

the primary mechanism. The power distributions within the selected patches in Fig. 6 are also shown in Fig. 7. It can be seen that the proposed methods, Algorithm 1 and Algorithm 2, produced very similar results to the Y4R in terms of extracted surface and double-bounce scattering power. The FDD and NNED-RS give relatively smaller surface scattering estimate, possibly due to slight azimuth slope modulation.

D. Study Scene 4: Terrains with Azimuth Slopes

Note by deriving (23) in Section III-C, we have in fact proposed another orientation angle estimation method that is different to the circular-polarization method [17] or the cross-pol minimization method [7]. In this subsection, we evaluate the estimated orientation angle in (23) for tilted terrains with azimuth slopes. The test L-band dataset is acquired by AIRSAR over Camp Roberts (California, US) in May 1998. For reducing the speckle effect we perform a simple boxcar filtering with a 3×3 window. The orientation angle estimated by (23) is shown in Fig. 8(a) whereas for comparison the orientation angle estimated by the circular-polarization method [17] is shown Fig. 8(b). It can be shown that Fig. 8(a) is similar to Fig. 8(b) but it is also much noisier. This is because our solution tries to fit an ideal model (ideal rotated Bragg scatterer) to the noisy data and so is more susceptible to speckle noise than the circular-polarization method. Nevertheless, Fig. 8(a) contains useful information which helps the decomposition

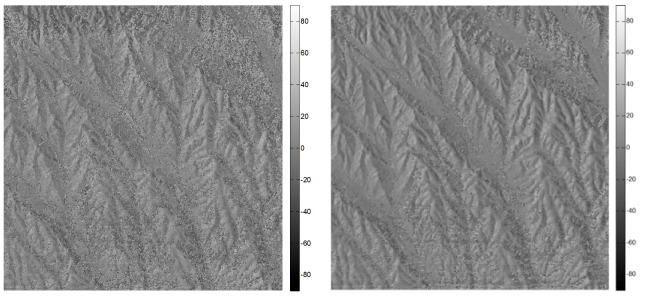

(a) (b)

Fig. 8. Orientation angles of the L-band AIRSAR data of Camp Roberts (California, US) estimated by (a) Eq. (23), and (b) circular-polarization method.

algorithm to discriminate tilted scatterers.

V. Conclusion

In this paper, we have shown that the POLSAR coherency matrix data can be completely decomposed into three components that are contributed by volume scattering and two single scatterers. In particular, under this scheme, the first important result is that the volume scattering power can be uniquely determined and it is equal to the minimum generalized eigenvalue of (9). Furthermore, we have pointed out that discrimination of the two single scatterers from the remaining matrix is ambiguous because more unknowns than independent equations are to be dealt with. Thus for single scatterer extraction, we have proposed two different approaches. The first one is based on simple eigendecomposition while the second one is based on optimal model fitting. Experimental results showed that both methods are able to properly differentiate surface and double-bounce scattering from the real POLSAR data.

Another important remark is the link between the proposed decomposition with NNED. It has been pointed out in Section III-A that the derived volume scattering power can be considered as the maximum value possible from the NNED perspective. Thus Algorithm 1 and Algorithm 2 are both special solutions of the NNED without assuming reflection symmetry and using the maximum amount of volume scattering. Although it is nevertheless legitimate to use a smaller volume power which consequently leads to a four-component model, the three-component model as used in this paper provides the simplest and most compact explanation of the polarimetric data.

Appendix A

In this appendix, we show that for any volume model generated from a cloud of random oriented scatterers, the corresponding coherency matrix is positive-definite in general. Suppose the Pauli-vector of the elementary scatterer is $\mathbf{k} = [k_1, k_2, k_3]^{\mathrm{T}}$, then the volume matrix can be derived as:

$$\mathbf{T}_{\mathrm{V}} = \mathbb{E}_\theta \left\{ \mathbf{T}(\theta) \right\} = \mathbb{E}_\theta \left\{ \mathbf{R}(\theta) \mathbf{k} \mathbf{k}^{\mathrm{H}} \mathbf{R}^{\mathrm{H}}(\theta) \right\} \tag{A.1}$$

where $\mathbb{E}_\theta$ denotes the mathematical expectation over θ; $\mathbf{R}(\theta)$ is the rotation matrix given in (19). Then for any non-zero vector $\mathbf{x} = [x_1, x_2, x_3]^{\mathrm{H}}$, the quadratic form of $\mathbf{T}_{\mathrm{V}}$ is:

$$\mathbf{x}^{\mathrm{H}} \mathbf{T}_{\mathrm{V}} \mathbf{x} = \mathbb{E}_\theta \left\{ |\mathbf{x}^{\mathrm{H}} \mathbf{R}(\theta) \mathbf{k}|^2 \right\} = \int_0^{2\pi} g(\theta) p(\theta) d\theta, \tag{A.2}$$

where $p(\theta)$ is the probability density function (pdf) of the orientation angles and $g(\theta)$ is given by:

$$g(\theta) = |k_1 x_1 + (k_2 x_2 + k_3 x_3) \cos 2\theta + (k_3 x_2 - k_2 x_3) \sin 2\theta|^2. \tag{A.3}$$

Note that $g(\theta) = 0$ has at most (in the worst case, zero) two solutions, θ_0 and $\theta_0 + \pi$, within $[0, 2\pi]$. Thus unless all the mass of $p(\theta)$ is only concentrated on these two points, i.e., unless $p(\theta)$ takes the singular form of $[\delta(\theta - \theta_0) + \delta(\theta - \theta_0 - \pi)]/2$ (where $\delta(\theta)$ is the Dirac delta function), we can always find a small neighborhood $\Delta \subset [0, 2\pi]$ such that $g(\theta) > 0, p(\theta) > 0$ for any $\theta \in \Delta$. Consequently, (A.2) becomes:

$$\mathbf{x}^{\mathrm{H}} \mathbf{T}_{\mathrm{V}} \mathbf{x} = \int_0^{2\pi} g(\theta) p(\theta) d\theta \geq \int_{\theta \in \Delta} g(\theta) p(\theta) d\theta. \tag{A.4}$$

The aforementioned equation demonstrates that $\mathbf{T}_{\mathrm{V}}$ will be generally positive-definite. The exception happens when $p(\theta) = [\delta(\theta - \theta_0) + \delta(\theta - \theta_0 - \pi)]/2$. However, in this case all the elementary scatterers will be aligned along the same direction θ_0. Such a volume model does not represent random scattering and so is excluded from discussion.

Appendix B

Suppose $\mathbf{A}$ and $\mathbf{B}$ are two 3×3 Hermitian matrices and $\mathbf{B}$ is positive-definite. We show that $\det(\mathbf{A} - x\mathbf{B}) = 0$ is a cubic equation with respect to x. In fact, $\det(\mathbf{A} - x\mathbf{B}) = 0$ can be written as:

$$a_3 x^3 + a_2 x^2 + a_1 x + a_0 = 0, \tag{B.1}$$

where the coefficients are given by:

$$\begin{aligned} a_0 =& A_{11}A_{22}A_{33} + 2\mathrm{Re}\{A_{13}A_{12}^*A_{23}^*\} \\ & - A_{11}|A_{23}|^2 - A_{22}|A_{13}|^2 - A_{33}|A_{12}|^2, \end{aligned} \tag{B.2a}$$

$$\begin{aligned} a_1 =& - B_{11}A_{22}A_{33} - B_{22}A_{11}A_{33} - B_{33}A_{11}A_{22} \\ & - 2\mathrm{Re}\{B_{12}A_{23}A_{13}^*\} - 2\mathrm{Re}\{B_{23}A_{12}A_{13}^*\} \\ & - 2\mathrm{Re}\{B_{13}A_{12}^*A_{23}^*\} + 2\mathrm{Re}\{B_{13}A_{22}A_{13}^*\} \\ & + 2\mathrm{Re}\{B_{23}A_{11}A_{23}^*\} + 2\mathrm{Re}\{B_{12}A_{33}A_{12}^*\} \\ & + B_{11}|A_{23}|^2 + B_{22}|A_{13}|^2 + B_{33}|A_{12}|^2, \end{aligned} \tag{B.2b}$$

$$\begin{aligned} a_2 =& A_{11}B_{22}B_{33} + A_{22}B_{11}B_{33} + A_{33}B_{11}B_{22} \\ & + 2\mathrm{Re}\{A_{12}B_{23}B_{13}^*\} + 2\mathrm{Re}\{A_{23}B_{12}B_{13}^*\} \\ & + 2\mathrm{Re}\{A_{13}B_{12}^*B_{23}^*\} - 2\mathrm{Re}\{A_{13}B_{22}B_{13}^*\} \\ & - 2\mathrm{Re}\{A_{23}B_{11}B_{23}^*\} - 2\mathrm{Re}\{A_{12}B_{33}B_{12}^*\} \\ & - A_{11}|B_{23}|^2 - A_{22}|B_{13}|^2 - A_{33}|B_{12}|^2, \end{aligned} \tag{B.2c}$$

$$\begin{aligned} a_3 =& - B_{11}B_{22}B_{33} - 2\mathrm{Re}\{B_{13}B_{13}^*B_{23}^*\} \\ & + B_{11}|B_{23}|^2 + B_{22}|B_{13}|^2 + B_{33}|B_{12}|^2, \end{aligned} \tag{B.2d}$$

Note that $\mathbf{B}$ is positive-definite and so $a_3 = -\det(\mathbf{B}) \neq 0$. Hence (B.1) is a cubic equation. Furthermore, define the following two constants:

$$P = \sqrt{(2a_2^3 - 9a_3a_2a_1 + 27a_3^2a_0)^2 - 4(a_2^2 - 3a_3a_1)^3}, \tag{B.3a}$$

$$Q = \sqrt[3]{(P + 2a_2^3 - 9a_3a_2a_1 + 27a_3^2a_0)/2}. \tag{B.3b}$$

Then the three roots of (B.1) are respectively given by:

$$x_1 = -\frac{a_2}{3a_3} - \frac{Q}{3a_3} - \frac{a_2^2 - 3a_3a_1}{3a_3Q}, \tag{B.4a}$$

$$x_2 = -\frac{a_2}{3a_3} + \frac{Q(1+j\sqrt{3})}{6a_3} + \frac{(1-j\sqrt{3})(a_2^2 - 3a_3a_1)}{6a_3Q}, \tag{B.4b}$$

$$x_3 = -\frac{a_2}{3a_3} + \frac{Q(1-j\sqrt{3})}{6a_3} + \frac{(1+j\sqrt{3})(a_2^2 - 3a_3a_1)}{6a_3Q}. \tag{B.4c}$$

APPENDIX C

In this appendix, we prove that for any positive-semidefinite Hermitian matrix $\mathbf{T}$ and any positive-definite Hermitian matrix $\mathbf{T}_{\mathrm{V}}$, all the generalized eigenvalues of (9) are non-negative. First we show that this generalized eigenvalue problem can be reduced to a standard (Hermitian) symmetric eigenvalue problem. Note that for any positive-definite Hermitian matrix $\mathbf{T}_{\mathrm{V}}$, by eigendecomposition it can be written as:

$$\mathbf{T}_{\mathrm{V}} = \mathbf{V}\mathbf{\Sigma}\mathbf{V}^{\mathrm{H}} = \mathbf{M}\mathbf{M}^{\mathrm{H}}, \tag{C.1}$$

where $\mathbf{\Sigma}$ is a diagonal matrix containing the eigenvalues of $\mathbf{T}_{\mathrm{V}}$, $\mathbf{V}$ is a unitary matrix, and $\mathbf{M} = \mathbf{V}\mathbf{\Sigma}^{\frac{1}{2}}$. Substituting (C.1) into (9) we have:

$$\mathbf{T}\mathbf{x} = \lambda\mathbf{M}\mathbf{M}^{\mathrm{H}}\mathbf{x}. \tag{C.2}$$

Since $\mathbf{T}_{\mathrm{V}}$ is positive-definite, $\mathbf{M}^{-1}$ and $\left(\mathbf{M}^{\mathrm{H}}\right)^{-1}$ exist. Then by multiplying $\mathbf{M}^{-1}$ on both sides of (C.2) and letting $\mathbf{y} = \mathbf{M}^{\mathrm{H}}\mathbf{x}$, we obtain:

$$\mathbf{M}^{-1}\mathbf{T}\left(\mathbf{M}^{\mathrm{H}}\right)^{-1}\mathbf{y} = \lambda\mathbf{y}. \tag{C.3}$$

Consequently, the generalized eigenvalues of (9) are also the eigenvalues of the Hermitian matrix $\mathbf{M}^{-1}\mathbf{T}\left(\mathbf{M}^{\mathrm{H}}\right)^{-1}$. In addition, it is easy to verify that $\mathbf{M}^{-1}\mathbf{T}\left(\mathbf{M}^{\mathrm{H}}\right)^{-1}$ is also positive-semidefinite. As a matter of fact, note that $\mathbf{T}$ is positive-semidefinite and for any vector $\mathbf{z}$:

$$\mathbf{z}^{\mathrm{H}}\left[\mathbf{M}^{-1}\mathbf{T}\left(\mathbf{M}^{\mathrm{H}}\right)^{-1}\right]\mathbf{z} = \mathbf{w}^{\mathrm{H}}\mathbf{T}\mathbf{w} \geq 0, \tag{C.4}$$

where $\mathbf{w} = \left(\mathbf{M}^{\mathrm{H}}\right)^{-1}\mathbf{z}$. So $\mathbf{M}^{-1}\mathbf{T}\left(\mathbf{M}^{\mathrm{H}}\right)^{-1}$ is positive-semidefinite. Thus equivalently, all the generalized eigenvalues of (9) are non-negative.

APPENDIX D

In this appendix, we prove that if P_{V} is equal to one of the generalized eigenvalues of (9), then $\mathbf{T} - P_{\mathrm{V}}\mathbf{T}_{\mathrm{V}}$ is positive-semidefinite if and only if P_{V} equals the minimum generalized eigenvalue of (9). According to Appendix C, the generalized eigenvalues of (9) are also those of the positive-semidefinite Hermitian matrix $\mathbf{M}^{-1}\mathbf{T}\left(\mathbf{M}^{\mathrm{H}}\right)^{-1}$. Then by eigendecomposition of $\mathbf{M}^{-1}\mathbf{T}\left(\mathbf{M}^{\mathrm{H}}\right)^{-1}$ we have:

$$\mathbf{M}^{-1}\mathbf{T}\left(\mathbf{M}^{\mathrm{H}}\right)^{-1} = \mathbf{U}\begin{bmatrix}\lambda_1 & 0 & 0\\ 0 & \lambda_2 & 0\\ 0 & 0 & \lambda_3\end{bmatrix}\mathbf{U}^{\mathrm{H}}, \tag{D.1}$$

where without loss of generality we assume $\lambda_1 \geq \lambda_2 \geq \lambda_3 \geq 0$; $\mathbf{U}$ is a unitary matrix. Consequently,

$$\mathbf{T} = \mathbf{M}\mathbf{U}\begin{bmatrix}\lambda_1 & 0 & 0\\ 0 & \lambda_2 & 0\\ 0 & 0 & \lambda_3\end{bmatrix}\mathbf{U}^{\mathrm{H}}\mathbf{M}^{\mathrm{H}}, \tag{D.2}$$

According to (D.2) and (C.1), we have:

$$\mathbf{T} - P_{\mathrm{V}}\mathbf{T}_{\mathrm{V}} = \mathbf{M}\mathbf{U}\begin{bmatrix}\lambda_1 - P_{\mathrm{V}} & 0 & 0\\ 0 & \lambda_2 - P_{\mathrm{V}} & 0\\ 0 & 0 & \lambda_3 - P_{\mathrm{V}}\end{bmatrix}\mathbf{U}^{\mathrm{H}}\mathbf{M}^{\mathrm{H}}, \tag{D.3}$$

From the above equation, it is easy to see that $\mathbf{T} - P_{\mathrm{V}}\mathbf{T}_{\mathrm{V}}$ is positive-semidefinite if and only if P_{V} is equal to λ_3, i.e., the minimum eigenvalue.

APPENDIX E

In this appendix, we derive the orientation angle in the Huynen decomposition. Let $\mathbf{S}$ be the scattering matrix. We first obtain the Graves matrix by $\mathbf{G} = \mathbf{S}^{\mathrm{H}}\mathbf{S}$. Then by eigendecomposition of $\mathbf{G}$ we have:

$$\mathbf{G} = \mathbf{S}^{\mathrm{H}}\mathbf{S} = \mathbf{U}\mathbf{\Lambda}\mathbf{U}^{\mathrm{H}}, \tag{E.1}$$

where $\mathbf{\Lambda} = \mathrm{diag}\{\lambda_1, \lambda_2\}$ are the eigenvalues and $\mathbf{U} = [\mathbf{u}_1, \mathbf{u}_2]$ are the corresponding eigenvectors. Without loss of generality, we assume $\lambda_1 \geq \lambda_2$ such that $\mathbf{u}_1$ represents the maximum transmitter polarization. The orientation angle τ of $\mathbf{S}$ is then defined as the orientation angle of $\mathbf{u}_1$. Specifically, Let the Jones-vector expression of $\mathbf{u}_1$ be:

$$\mathbf{u}_1 = \begin{bmatrix}E_x\\ E_y e^{j\phi}\end{bmatrix}. \tag{E.2}$$

The orientation angle τ is thus given by:

$$\tau = \frac{1}{2}\left(\tan^{-1}\frac{2E_xE_y\cos\phi}{E_x^2 - E_y^2} + k\pi\right), \tag{E.3}$$

where k ensures that $\tau \in \left[-\frac{\pi}{2}, \frac{\pi}{2}\right]$ and that $\sin 2\tau$ and $\cos\phi$ are of the same sign.

APPENDIX F

In this appendix we derive the orientation angle θ that maximizes P_{S} in (21a). The optimization problem is:

$$\max_{\theta}\left\{T'_{11}(\theta) + T'_{22}(\theta) - \frac{|T'_{13}(\theta)|^2 + |T'_{23}(\theta)|^2}{T'_{33}(\theta)}\right\}, \tag{F.1}$$

where $T'_{ij}(\theta)$ are the elements of the rotated matrix $\mathbf{T}'(\theta) = \mathbf{R}(\theta)\mathbf{T}'\mathbf{R}^{\mathrm{T}}(\theta)$ and $\mathbf{R}(\theta)$ is given in (19). By writing $T'_{ij}(\theta)$ in terms of T'_{ij} and θ, the above optimization problem is equivalent to:

$$\max_{\theta}\left\{\frac{a\cdot\cos 4\theta + b\cdot\sin 4\theta + c}{d\cdot\cos 4\theta + e\cdot\sin 4\theta + f}\right\}, \tag{F.2}$$

where the constants a, b, c, d, e, f are given in (24). Let

$$\frac{a\cdot\cos 4\theta + b\cdot\sin 4\theta + c}{d\cdot\cos 4\theta + e\cdot\sin 4\theta + f} = x. \tag{F.3}$$

Then we have:

$$(dx - a)\cdot\cos 4\theta + (ex - b)\cdot\sin 4\theta = c - fx. \tag{F.4}$$

According to (F.4) and Cauchy inequality, for any θ the following relation holds:

$$(dx-a)^2+(ex-b)^2 \leq (c-fx)^2. \tag{F.5}$$

Thus the range of x can be solved from the following quadratic inequality:

$$x^2 - Bx + C \leq 0, \tag{F.6}$$

where the constants B and C are given by (24a)–(24b). According to (F.6), the maximum value for x is:

$$x_{\max} = B + \sqrt{B^2 - C}. \tag{F.7}$$

Then substituting $x_{\max}$ in (F.4) the rotational angle can be obtained with the following equations:

$$\cos 4\theta = \frac{\left(B+\sqrt{B^2-C}\right)d - a}{c - \left(B+\sqrt{B^2-C}\right)f}, \tag{F.8a}$$

$$\sin 4\theta = \frac{\left(B+\sqrt{B^2-C}\right)e - b}{c - \left(B+\sqrt{B^2-C}\right)f}. \tag{F.8b}$$

Finally, (F.8) leads to (23).

ACKNOWLEDGMENT

The authors would like to thank the editor, associate editor, and the anonymous reviewers for their invaluable comments to improve the quality of this paper.

REFERENCES

[1] S.R. Cloude and E. Pottier, "A review of target decomposition theorems in radar polarimetry," *IEEE Trans. Geosci. Remote Sens.*, vol. 34, no. 2, pp. 498-518, Mar. 1996.

[2] A. Freeman and S.L. Durden, "A three-component scattering model for polarimetric SAR data, *IEEE Trans. Geosci. Remote Sens.*, vol. 36, no. 3, pp. 963-973, May 1998.

[3] Y. Yamaguchi, T. Moriyama, M. Ishido, and H. Yamada, "Four-component scattering model for polarimetric SAR image decomposition, *IEEE Trans. Geosci. Remote Sens.*, vol. 43, no. 8, pp. 1699-1706, Aug. 2005.

[4] W. An, Y. Cui, and J. Yang, "Three-component model-based decomposition for polarimetric SAR data, *IEEE Trans. Geosci. Remote Sens.*, vol. 48, no. 6, pp. 2732-2739, June 2010.

[5] J.J. van Zyl, M. Arii, and Y. Kim, "Model-based decomposition of polarimetric SAR covariance matrices constrained for nonnegative eigenvalues, *IEEE Trans. Geosci. Remote Sens.*, vol. 49, no. 9, pp. 1104-1113, Sept. 2011.

[6] M. Arii, J.J. van Zyl, and Y. Kim, "Adaptive model-based decomposition of polarimetric SAR covariance matrices, *IEEE Trans. Geosci. Remote Sens.*, vol. 49, no.3, pp. 1104-1113, Mar. 2011.

[7] Y. Yamaguchi, A. Sato, W.M. Boerner, R. Sato, and H. Yamada, "Four-component scattering power decomposition with rotation of coherency matrix, *IEEE Trans. Geosci. Remote Sens.*, vol. 49, no. 6, pp. 2251-2258, June 2011.

[8] Y. Yamaguchi, G. Singh, S.-E. Park, and H. Yamada, "Scattering power decomposition using fully polarimetric information, in *Proc. IGARSS*, Munich, July 2012.

[9] J.-S. Lee and T.L. Ainsworth, "The effect of orientation angle compensation on coherency matrix and polarimetric target decompositions, *IEEE Trans. Geosci. Remote Sens.*, vol. 49, no. 1, pp. 53-64, Jan. 2011.

[10] J.-S. Lee, M.R. Grunes, and G. de Grandi, "Polarimetric SAR speckle filtering and its implication for classification, *IEEE Trans. Geosci. Remote Sens.*, vol. 37, no. 5, pp. 2363-2373, Sept. 1999.

[11] A. Freeman, "Fitting a two-component scattering model to polarimetric SAR data from forests, *IEEE Trans. Geosci. Remote Sens.*, vol. 45, no. 8, pp. 2583-2592, Aug. 2007.

[12] O. Antropov, Y. Rauste, and T. Hame, "Volume scattering modeling in PolSAR decompositions: study of ALOS PALSAR data over Boreal forest, *IEEE Trans. Geosci. Remote Sens.*, vol. 49, no. 10, pp. 3838-3848, Oct. 2011.

[13] Y. Cui, Y. Yamaguchi, J. Yang, S.-E. Park, H. Kobayashi, and G. Singh, "Three-component power decomposition for polarimetric SAR data based on adaptive volume scattering modeling, *Remote Sens.*, vol. 4, no. 6, pp. 1559-1572, May 2011.

[14] [Online]. http://en.wikipedia.org/wiki/Singular_value_decomposition.

[15] J.J. van Zyl, "Application of Cloudes target decomposition theorem to polarimetric imaging radar data, *Radar Polarimetry*, vol. SPIE-I748, pp. 184-212, 1992.

[16] J. R. Huynen, "Measurement of the target scattering matrix, *Proc. IEEE*, vo. 53, no. 8, pp. 936-946, 1969.

[17] J.-S. Lee, D.L. Schuler, and T.L. Ainsworth, "Polarimetric SAR data compensation for terrain azimuth slope variation, *IEEE Trans. Geosci. Remote Sens.*, vol. 38, no. 5, pp. 2153-2163, Sept. 2000.

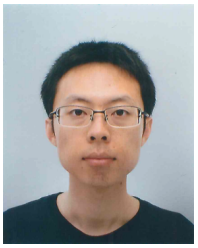

Yi Cui (S'09–M'11) received the B.S. degree (with honors) in electronic information science and technology from the College of Electronic Science and Engineering of Jilin University, Changchun, China, in 2006. From 2006 to 2011 he was a doctoral student at Tsinghua University, Beijing, China and received the Ph.D. degree in information and communication engineering from the Department of Electronic Engineering of Tsinghua University in 2011. He is currently a post-doctoral research fellow at Niigata University, Japan.

Dr. Cui is the first-prize winner of the student paper competition at the 2010 Asia-Pacific Radio Science Conference (AP-RASC10) in Toyama, Japan. He has also the recipient of the Best Paper Award of the 2012 International Symposium on Antennas and Propagation (ISAP). His research interests include signal and image processing and their applications in SAR remote sensing, radar polarimetry, and electromagnetic theory.

Yoshio Yamaguchi (M'83–SM'94–F'02) received the B. E. degree in electronics engineering from Niigata University, Niigata, Japan, and the M. E. and Dr. Eng. degrees from the Tokyo Institute of Technology, Tokyo, Japan, in 1976, 1978, and1983, respectively.

In1978, he joined the Faculty of Engineering, Niigata University, where he is a Professor. From 1988 to 1989, he was a Research Associate at the University of Illinois at Chicago. His interests are in the field of radar polarimetry, microwave sensing, and imaging.

Dr. Yamaguchi was Chair of the IEEE Geoscience and Remote Sensing Society Japan Chapter (20022003), Vice Chair (20002001), organizer of Polarimetric-Synthetic Aperture Radar Workshops (20002005) in Japan, and Associate Editor for Asian affairs of the GRSS Newsletter since 2003. He is a Fellow of the Institute of Electronics, Information and Communication Engineers, Japan, and was the recipient of the 2008 IEEE GRSS Education Award.

Jian Yang (M'98–SM'02) received the B.S. and M.S. degrees from Northwestern Polytechnical University, Xian, China, in 1985 and 1990, respectively, and the Ph.D. degree from Niigata University, Niigata,Japan, in 1999.

In 1985, he joined the Department of Applied Mathematics, Northwestern Polytechnical University. From 1999 to 2000, he was an Assistant Professor with Niigata University. In April 2000, he joined the Department of Electronic Engineering, Tsinghua University, Beijing, China, where he is now a Professor. His interest includes radar polarimetry, remote sensing, mathematical modeling, optimization in engineering, and Fuzzy theory. Dr. Yang is the chairman of IEICE in Beijing area and the vice-chairman of IEEE AES in Beijing chapter.

Hirokazu Kobayashi (M'87–SM'10) was born in Hokkaido, Japan, on 1955. He received the B.E.E. and M.E.E. degrees from the Shizuoka University, Shizuoka, Japan in 1978, 1980, respectively.

He joined Fujitsu LTD., Kawasaki, Japan at 1980. Since 1981 he has been with the Fujitsu System Integration Laboratories as a Researcher on developments for micro/millimeter wave wide-band antennas, active phased array systems and theoretical investigation for scattering cross sections. During 1999-2010, he served as General Manager of the laboratories and Fujitsu LTD. He received the Dr. Eng. degree from Tsukuba University, Tsukuba, Japan, in 2000. From 2010 he joined the Faculty of Engineering as a Professor in Niigata University, Niigata, Japan. His current research interests are high-frequency analysis for computing of radar cross-section of large objects and near-field analysis using physical optics/physical theory of diffraction/geometrical theory of diffraction (PO/PTD/GTD), and near-field transformation to far-field based on microwave imaging theory (SAR/ISAR).

Dr. Kobayashi is a member of the Institute of Electronics, Information and Communication Engineers, Japan.

Sang-Eun Park (S'05–M'07) received the B.S. and M.S. degrees in geophysics and Ph.D. degree in radar remote sensing and geophysics from the Seoul National University, Seoul, Korea, in 2000, 2002, and 2007 respectively. From 2007 to September 2009, he worked at the Radar Polarimetry Remote Sensing Group of the University of Rennes 1, Rennes, France, for a post-doctoral fellow on radar polarimetry. From October 2009 to January 2010, he was a project assistant in the Institute of Photogrammetry and Remote Sensing, Vienna University of Technology, Vienna, Austria. He is currently an Assistant Professor in the Graduate School of Science and Technology at Niigata University, Japan. His research interests include polarimetric SAR classification, forward and Inverse modeling of microwave vegetation and surface backscattering, and investigation of multi-source data integration methodology.

Gulab Singh (S'09–M'11) received his B.Sc. and M.Sc. degrees in physics from the Meerut University, Meerut, India in 1998 and 2000, respectively, and his M. Tech. degree in remote sensing from the Birla Institute of Technology, Ranchi, India in 2005 and his Ph.D. from Indian Institute of Technology Bombay, Mumbai, India in 2010. He taught Physics to intermediate students for an academic session in 2002-2003 at Janta Inter College, Jhabiran, Saharanpur, India and from 2005 to 2007, he was Research Fellow at Indian Institute of Technology Bombay, Mumbai, India, where he was involved in several research projects related to POL-SAR and In-SAR data analysis for snow and ice parameters retrieval. He is currently Post Doctoral Fellow at Graduate School of Science and Technology, Niigata University, Niigata, Japan. His current research interests include SAR data analysis, SAR polarimetry and SAR interferometry techniques development for earth and lunar surface parameters estimation.